ECN-C--91-061

SEPTEMBER 1991

NL92C0236

ECN
energy innovation

FINITE ELEMENT ANALYSES OF A HEATER-INTERRUPTION IN THE HAW TEST FIELD

B.A. VAN DEN HORN

The Netherlands Energy Research Foundation ECN is the leading institute in the Netherlands for energy research. ECN carries out pure and applied research in the fields of nuclear energy, fossil fuels, renewable energy sources, environmental aspects of energy supply, computer science and the development and application of new materials. Energy studies are also a part of the research programme.

ECN employs more than 900 staff. Contracts are obtained from the government and from national and foreign organizations and industries.

ECN's research results are published in a number of report series, each series serving a different public from contractors to the international scientific world.

The C-series is for contract reports that contain the results of contract research. The contractor's name can be found on page 2.

Netherlands Energy Research Foundation ECN
Service Unit General Services
P.O. Box 1
NL-1755 ZG Petten
The Netherlands
Telephone: +31 2246 43 23
Fax . +31 2246 34 83

This report is available on remittance of Dfl. 20 to:
ECN, SU General Services, Petten,
The Netherlands.
Giro account (postal account) No. 3977703.
Please quote the report number.

SEPTEMBER 1991

ECN-C--91-061

FINITE ELEMENT ANALYSES OF A HEATER-INTERRUPTION IN THE HAW TEST FIELD

B.A. VAN DEN HORN

This work has been performed under contract No. Fl-1W-0003-D(B) in the framework of the Commission of the European Communities R&D Programme on Management and Storage of Radioactive Waste.

ABSTRACT

In this report the results of two finite element analyses of the HAW field are presented. The determination of the influence of a heater-interruption on the tube load as well as the differences in the evolution of the tube load for both types of boreholes (type A and type B) are the main objectives of this report. Axisymmetric models are made for both type of boreholes in order to simulate this heater-interruption. It appeared that a heater-interruption of 4 hours leads to a temperature drop of 17.2°C at the borehole wall and to a maximum reduction of the tube load of 1.76 MPa. About 20 days after reparation of the heaters the evolution of the maximum temperature and the maximum tube load will be rehabilitated; the difference with the corresponding evolutions due to an uninterrupted heat-production are negligible.

CONTENTS

LIST OF SYMBOLS

a	borehole radius, mm
A	constant in Norton's secondary creep law
b	external radius of the model, mm
c	inner steel radius, mm
c_p	specific heat, J/kg K
d	outer steel radius, mm
E	Young's modulus, MPa
F	force, N
h	height of the model, mm
r	radial coordinate, mm
n	exponent in Norton's secondary creep law
p	pressure, MPa
s	stress in the steel liner, MPa
t	time, days
T	temperature, °C
u	radial displacement, mm
$\hat{u}$	dimensionless radial displacement
Q	heat, W
V	volume, mm^3
w	axial displacement, mm
z	axial coordinate, mm
α	coefficient of thermal expansion, K^{-1}
β	stiffness-correction function
ε	strain
θ	circumferential coordinate, rad
λ	heat conductivity coefficient, W/m K
ν	Poisson ratio
ρ	density, kg/m^3
σ	stress, MPa
τ	dimensionless time

Superscripts

el	elastic
cr	creep
p	porous medium
s	steel

Subscripts

eq	equivalent
rr	radial
$\theta\theta$	tangential
zz	axial

1 INTRODUCTION

In the Asse salt mine the HAW experiment has been running since 1985. The HAW test field is located at a depth of 800m and consists of two large galleries each with a length of about 60m, a width of 10.5m and a height of 8m. The pillar between the galleries has a thickness of 10m. In the bottom of each of the galleries 4 vertical boreholes with a depth of 15m have been made. The spacing between the boreholes is 15m in the direction of the galleries and 19m crosswise. The arrangement of the galleries and boreholes is elucidated in Fig. 1.1 where a horizontal cross-section at the 800m level is given.

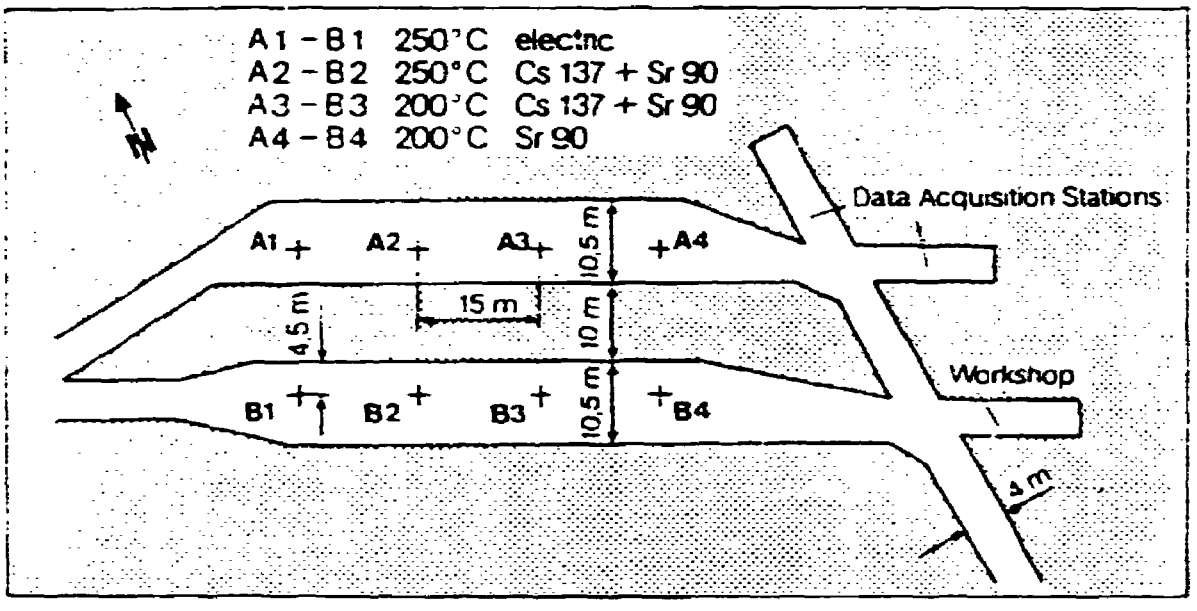

Figure 1.1 Arrangement of the boreholes in the HAW test field.

With electrical heaters heat was brought into the salt to investigate the thermo-mechanical behaviour of a salt formation [1,2]. In the boreholes of the HAW test field a lining of steel is placed in order to guarantee the continuous retrievability of the radio-active canisters over the complete testing period. This implies that the liner has been designed with the objective to provide mechanical strength against the thermally induced pressure load from the salt. Two types of boreholes are present in the test field. In the boreholes of type A the annular gap between the liner and borehole wall is backfilled with a porous medium consisting of ceramic aluminium beads in order to provide access to the water and gas components liberated on the entire heated and irradiated length of the borehole (cf. Fig. 1.2). In case of a type B borehole unrestricted convergence of the borehole wall and a creeping of the salt onto the liner is permitted due to a lack of backfilling.

In every type of borehole electrical heaters were placed. The two electrically heated boreholes have to be representative for the remaining six boreholes with radio-active sources during the whole time period of the experiments. Therefore, it was necessary to examine the consequences of an interruption of the heat production on the thermo-mechanical behaviour of the salt around the borehole [3]. In this report a more detailed study on the effects of a heater-interruption is presented. Axisymmetrical models are made of the boreholes of the A and B type in the HAW test field in order to find the thermally induced pressure load from the salt on the lining in the boreholes. The study of the influence of a heater-interruption on the temperatures and load acting on the tube is the main purpose of these analyses. The local stress distribution around the borehole is investigated in detail. The analyses are represented in several parts, viz:

1) Linear elastic solution
2) Isothermal creep analysis with an empty borehole until t = 675 days.
3) The borehole filled with the tube and an isothermal creep analysis until t = 680 days
4) Thermally accelerated creep analysis until t = 936.22 days
5) Heater-interruption of approximately 4 hours until t = 936.39 days
6) Thermally accelerated creep analysis until t = 1200 days

The internal heat generation will induce deformations in the salt. However, the displacements are only very small and of little effect to the temperature distribution. In view of this smallness a separate treatment of the thermal analysis from the structural analysis seems to be justified. In chapter 2 the thermal analysis is discussed. In chapter 3 a description of the structural analysis is presented. Chapter 4 deals with the solution of the thermal analysis and in chapter 5 the results of the structural analysis are given.

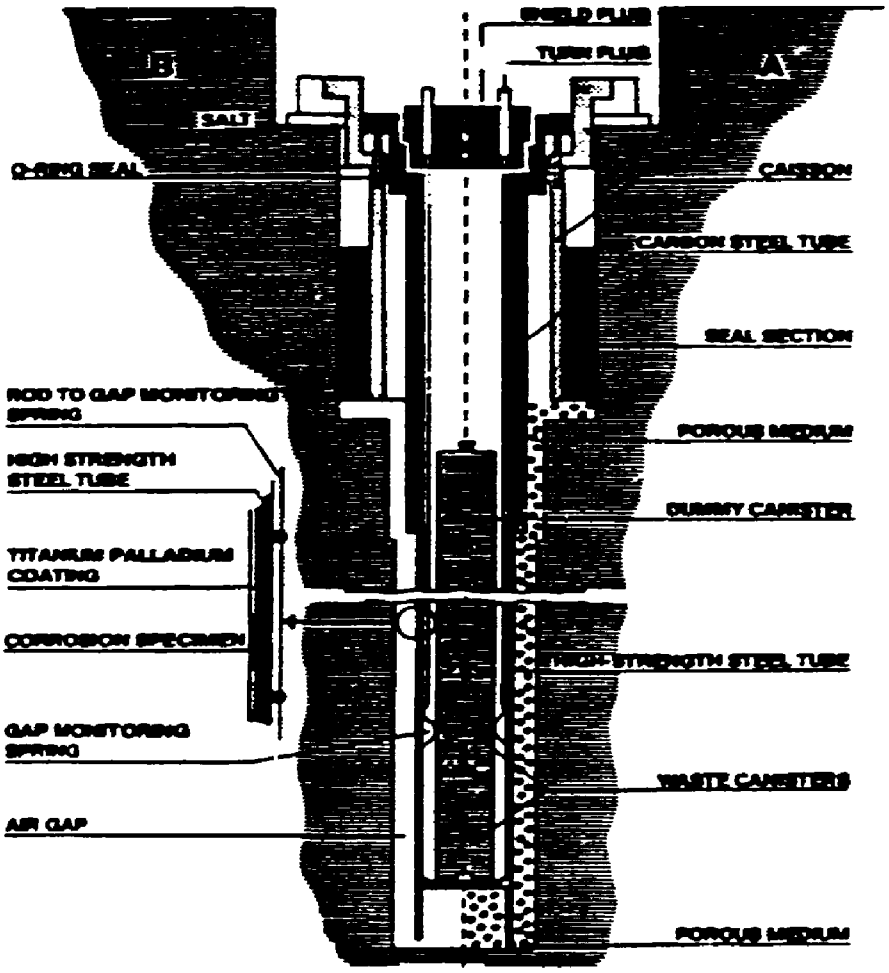

Figure 1.2 The boreholes, type A (right side) and type B (left side).

2 THERMAL ANALYSIS

2.1 Modelling assumptions

The temperature calculations are made with the computer code TASTE (Three-dimensional Analyses of Salt dome TEmperatures), developed at ECN [4]. The program is based on an analytical model of a continuous time-dependent point-source in an infinite solid of homogeneous isotropic material with temperature independent material properties. In the method of calculation the rock salt properties are assumed to be constant.
The model is an axisymmetrical simulation of one borehole in the HAW test field. The influence of the interaction of the boreholes is not taken into account, since the objective of the analyses is to find the thermally induced pressure load from the salt on the lining in the boreholes. This seems to be justified since the errors in the local stresses, strains and temperatures are expected to be small in the time period considered. The interaction of the borehole and the gallery is not included either. In Fig. 2.1 the geometry is schematically depicted. The radius of the borehole wall is denoted by a. The external radius b of the model is chosen approximately 25 times a, so that the boundaries of the configuration are considered to be at a sufficiently large distance of the borehole to represent the undisturbed salt at infinity. The inner and outer radius of the steel liner are denoted by c and d, respectively, while the height of the model is given by h.

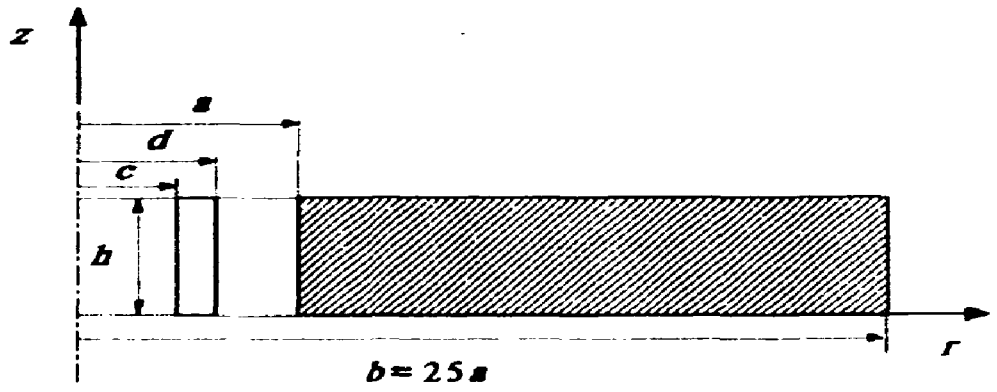

Figure 2.1 Definition of the coordinate system and the geometrical parameters of the model.

The heat source in a borehole of the HAW test field is an electrical heater with a length of 6 meters. The centre of the heat source is situated 12 meters below the gallery floor. Since the maximum load on the liner will occur at the centre of the heat source, temperatures are calculated in a horizontal plane at the centre of the heat source. The heater is considered to be composed of a number of point sources each with a finite source length. The sum of all the source lengths equals 6 m. In Fig. 2.2 the location of the calculation points and the heat source are depicted. It is obvious that the largest temperature and stress gradients occur close to the borehole wall. Therefore, to accurately describe the temperature gradient a high concentration of temperature calculation points is needed close to the borehole. At larger distances less calculation points will suffice. The radial coordinates r_i of the calculation points are chosen according to the relation

$$r_k = (1.1)^{k-1} a, \qquad k = 1,\ldots,N$$
$$r_k = d + k\,\frac{(d-c)}{2}, \qquad k = 0, -1, -2 \tag{1}$$

where N should be chosen as to establish the relation $b \approx 25\ a$. In this equation k is the number of the radial layer. The non-positive values denote the calculation points in the steel liner. The calculated temperatures will be used as input for the structural analysis. The calculated isothermal and thermally accelerated convergence of the borehole is very sensitive to the spatial distribution of the elements. It has been shown that a choice of 1.1 for the growth factor which defines the position of the calculation points for the temperature analysis (and the nodal points for the structural finite element analysis as will be presented in chapter 3) leads to an accurate solution for the coupled analysis [5]. The parameters that describe the temperature calculation points and the borehole geometry in the HAW test field are presented below (cf. Fig. 2.1 and 2.2):

$$a = 0.250\text{m}\ ,\quad c = 0.210\ \text{m}\ ,\ d = 0.228\text{m}\ ,\ h = 0.200\text{m}\ ,\ N = 48 \tag{2}$$

Temperatures are calculated in the plane $z = h/2$.

2.2 Boundary conditions

The convection and heat flow across the boundary of the model are zero. The initial temperature in the salt volume is 36°C. As temperature rises due to the presence of the heat source, conduction in radial direction will take place. The internal heat production of the glass canisters is taken constant:

$$Q = 9600\ \text{W} \tag{3}$$

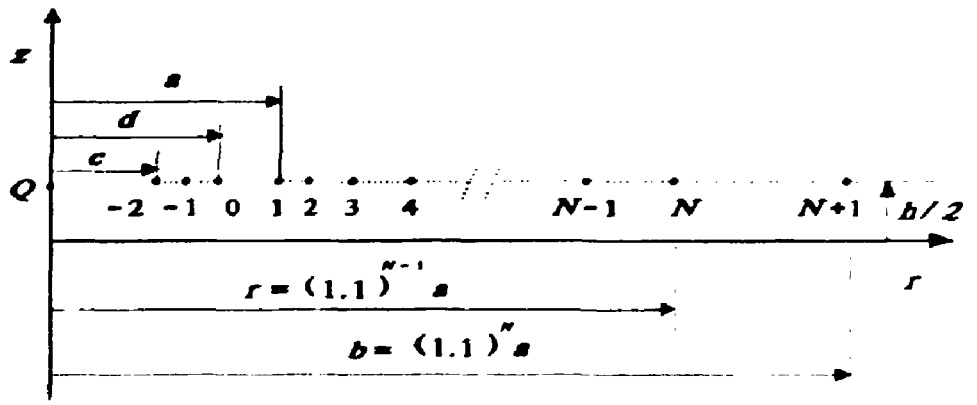

Figure 2.2 Definition of the temperature calculation points and the heat source.

2.3 Material properties

For the specific heat c_p of the salt the following formula is valid:

$$\rho c_p = 1870490 + 387.72\ T \quad [\mathrm{J / m^3 K}] \tag{4}$$

in which the temperature T is measured in K and ρ is the density of the salt. For the heat conductivity coefficient λ a cubical polynomial is generally used:

$$\lambda = 5.734 - 0.01838\ T + 2.86\ 10^{-5}\ T^2 - 1.51\ 10^{-9}\ T^3 \quad [\mathrm{W/m\ K}] \tag{5}$$

Since TASTE can only deal with homogeneous isotropic materials with temperature independent material properties the specific heat and heat conductivity coefficient are evaluated at a constant temperature T = 143°C (416 K). This is about half the maximum temperature that is expected to occur in the salt volume. In Table 2.1 the material properties are presented for the salt. The specific heat c_p, the heat conductivity coefficient λ and the density ρ for the steel are chosen equal to the corresponding salt properties to simplify the determination of the temperatures in the steel liner.

Table 2.1 Material properties for the salt.

ρc_p J/(m^3 K)	λ J/(day m K)
1925990	322340

3 STRUCTURAL ANALYSIS

3.1 Modelling assumptions

The structural analyses are performed for both the A and B type boreholes with the help of the finite element code ANSYS Rev 4.4a [6]. Schematical representations of the finite element meshes of the model for the structural analyses are given in Fig. 3.1.

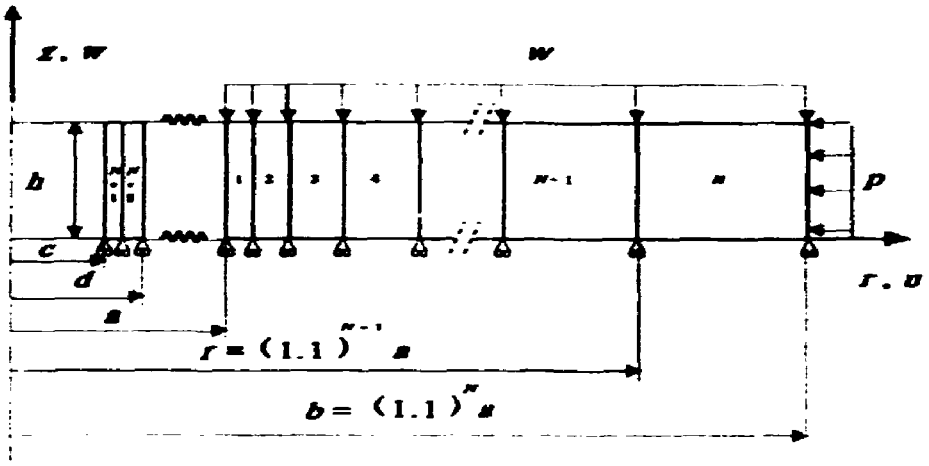

(a)

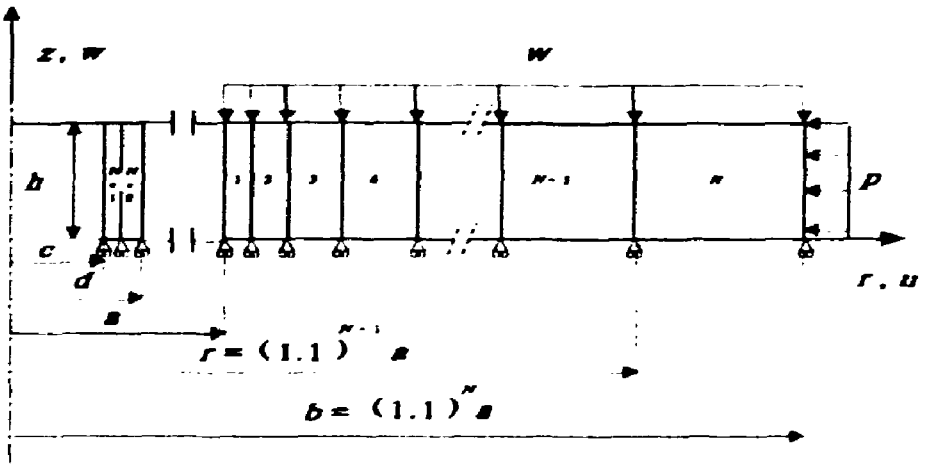

(b)

Figure 3.1 Finite element meshes for the A-type borehole (a) and the B-type borehole (b).

The radial coordinates of the nodal point correspond to the temperature calculation points as described in chapter 2. As has been previously stated, in the borehole of type A the annular gap between liner and borehole wall is backfilled with a porous medium consisting of ceramic aluminium beads in order to provide access to the water and gas components liberated on the entire heated and irradiated length of the borehole. In case of a type B borehole unrestricted convergence of the borehole wall and creeping of the salt onto the liner is possible due to a lack of backfilling. The effect of this backfilling on the maximum tube load can thus be studied.

3.2 Element type

The analysis is performed by using a 2-D isoparametric solid element for the salt and the steel. These elements have 4 corner nodes and are generally used for 2-D modelling of solid structures (STIFF42 of the ANSYS element-library). This element is used as an axisymmetric ring element. The mechanical behaviour of the porous medium is simulated by connecting the steel liner and the salt with non-linear force-deflection elements (STIFF39) in the case of the analysis of an A-type borehole. In case of a B-type boreholes a 2-D interface element (STIFF12) was used to describe the upkeep or break of the physical contact of the salt and the steel.

3.3 Temperature boundary conditions

An initial overall temperature of 36°C is selected. After 680 days the heat production is started and from this point of time the initial temperature distribution is replaced by the time dependent temperature distribution calculated with TASTE. Details about this separate thermal analysis are given in chapter 4.

3.4 Constitutive equations

The elastic properties of the salt are described by the Young's modulus and the Poisson ratio. The latter one is chosen as $\nu = .3$. In [5] it has been stated that the BGR recommends a Young's modulus $E = 25000$ MPa. However, a smaller ECN-value of $E = 7600$ MPa is used in order to include primary creep effects in accordance with [3,5,7]. The secondary creep is described by Norton's law:

$$\dot{\varepsilon}_{eq}^{cr} = A\,\sigma^{n}\exp(-e/T + e/314) \tag{6}$$

where $A = 8.8\ 10^{-11}$ MPa^{-n}/d, $n = 5.5$ and $e = 8250$ K, yielding

$$\dot{\varepsilon}_{eq}^{cr} = 22.6165\,\sigma^{5.5}\exp(-8250/T) \tag{7}$$

In full agreement with [7] initial thermal strains are excluded by setting the stress free temperature to the initial overall temperature $T = 36$°C ($T = 309$ K). The coefficient of thermal expansion is chosen as $\alpha = 4\ 10^{-5}$ K^{-1}. A Young's modulus $E_s = 2.1\ 10^{6}$ N/mm^2, a Poisson ratio $\nu_s = 0.3$ and a coefficient of thermal expansion $\alpha_s = 1.6\ 10^{-5}$ K^{-1} were selected for the steel liner. In the case of the A-type borehole the stiffness of the porous medium is dependent on the volume strain of the annular gap. A linear relation between Young's modulus E_p of the porous medium and the volume strain $\Delta V/V$ of the annular gap is assumed (cf. Fig. 3.2). In appendix A details about the simulation of this material behaviour are given.

3.5 Boundary conditions

The configuration represents a region at the centre of the stack of heaters. Which means that the upper boundary of the configuration would be located at 11.9m below the floor of the galleries in the HAW test field. A uniform lithostatic pressure of 11 MPa was taken based on the convergence results presented in [7]. At the horizontal boundaries this pressure is applied by imposing an axial displacement

$$w = \frac{(1-2\nu)}{E} ph = 0.12 \text{ mm}, \quad \text{for } Z = h$$
$$w = 0, \quad \text{for } Z = 0 \tag{8}$$

in the salt volume.

3.6 Control parameters

Since secondary creep is the only non-linear phenomenon in the analyses the control parameter for the time integration scheme can be chosen as high as stability limitations permit. The criterion

$$\Delta \varepsilon_{eq}^{cr} \leq 0.25\, \varepsilon_{eq}^{el} \tag{9}$$

is chosen for all time steps.

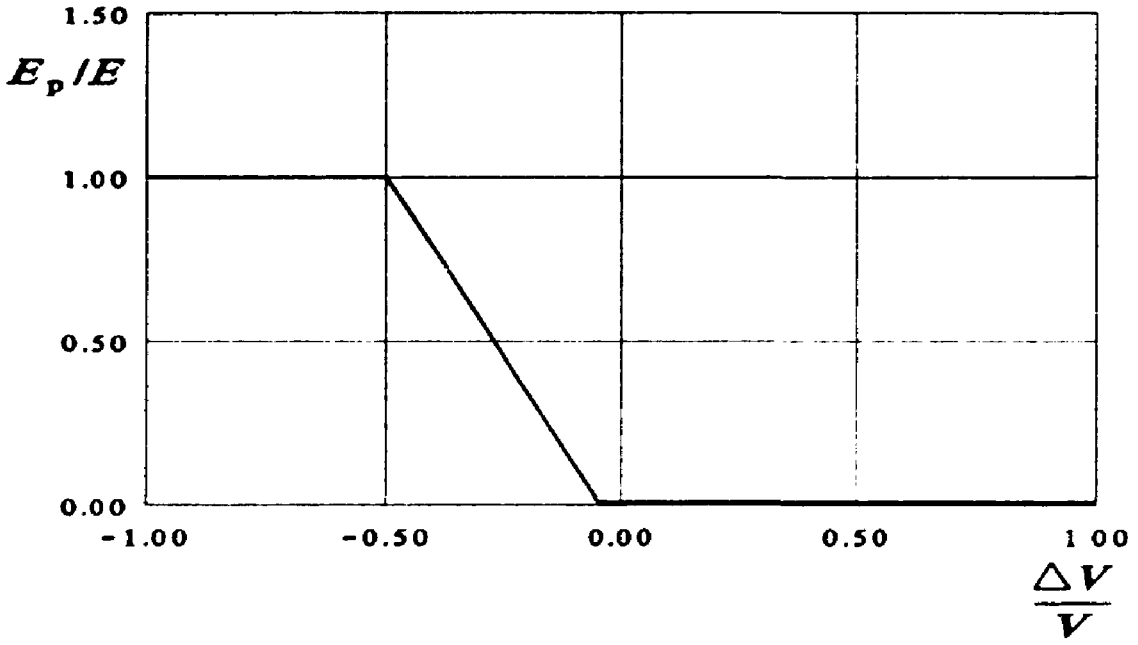

Figure 3.2 Stiffness E_p of the porous medium as a function of the volume strain $\Delta V/V$.

4 THE SOLUTION OF THE THERMAL ANALYSIS

The thermal analysis covers a period of 520 days starting at t = 680 days and ending at t = 1200 days. It starts with a uniform temperature of 36°C. The heat production was started after 680 days while after an operation period at t = 936.22 days the heater failed and was out of service for approximately 4 hours. During this period the power was reduced to zero so no heat was generated at all. At t = 936.39 days the heater was repaired and the same heat was produced.

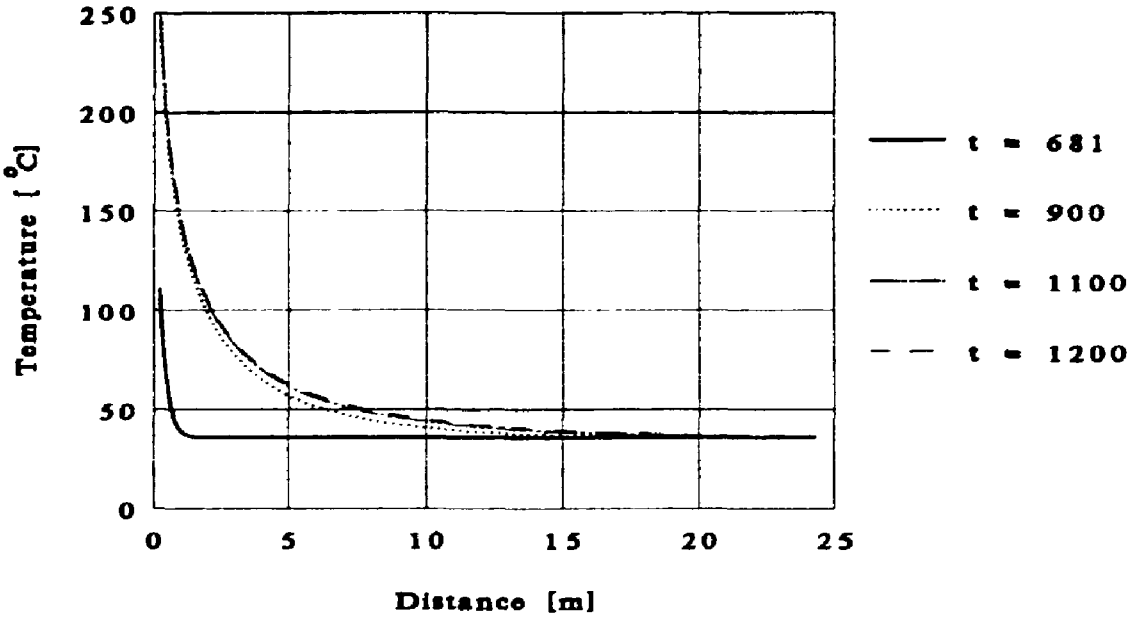

Figure 4.1 Temperature distribution for several points of time.

In Fig. 4.1 the temperature distribution is presented for several points of time. It is clear that the temperature rise is a time dependent phenomenon restricted to a relatively small region around the borehole. Apparantly, the time period considered is too small for the heat to reach the boundary $r = b$.

An extra temperature calculation for a continuous heat-production was made. These temperatures are tabulated in Table 4.1 and can be compared with the calculated temperatures at the moment of the heater-interruption. Fig. 4.1 presents the temperature evolution for several points of time. In Table 4.2 the numerical values of the temperatures at the borehole wall have been tabulated from the moment that the heater failed. The temperature at the borehole wall is 234.25°C the moment that the heater fails and a temperature drop of 17.2°C was found after 4 hours. After reparation of the heaters a maximum temperature of 240.49°C is reached. It appears that at a distance of more than 59 cm from the heat source the heater interruption is hardly noticed. This is also visible in Fig. 4.3 where the temperature distribution is presented at the begin, the end and shortly after the heater-interruption. At a distance of 59cm from the borehole the decrease in temperature due to the heater-interruption is only noticed after the reparation of the heaters.

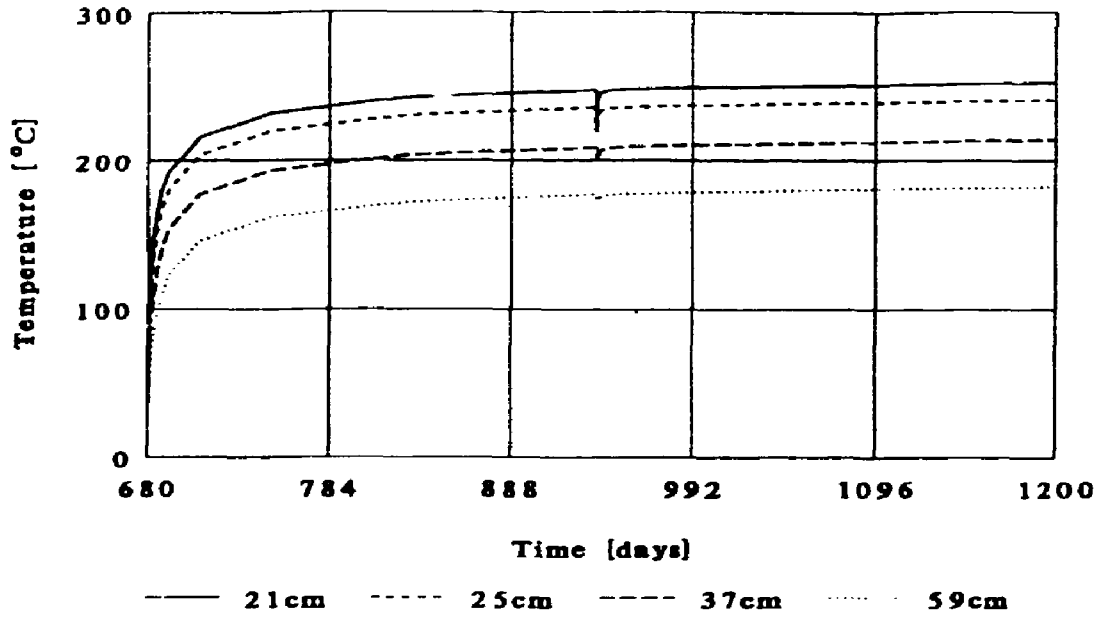

Figure 4.2 Temperature evolution for several calculation points.

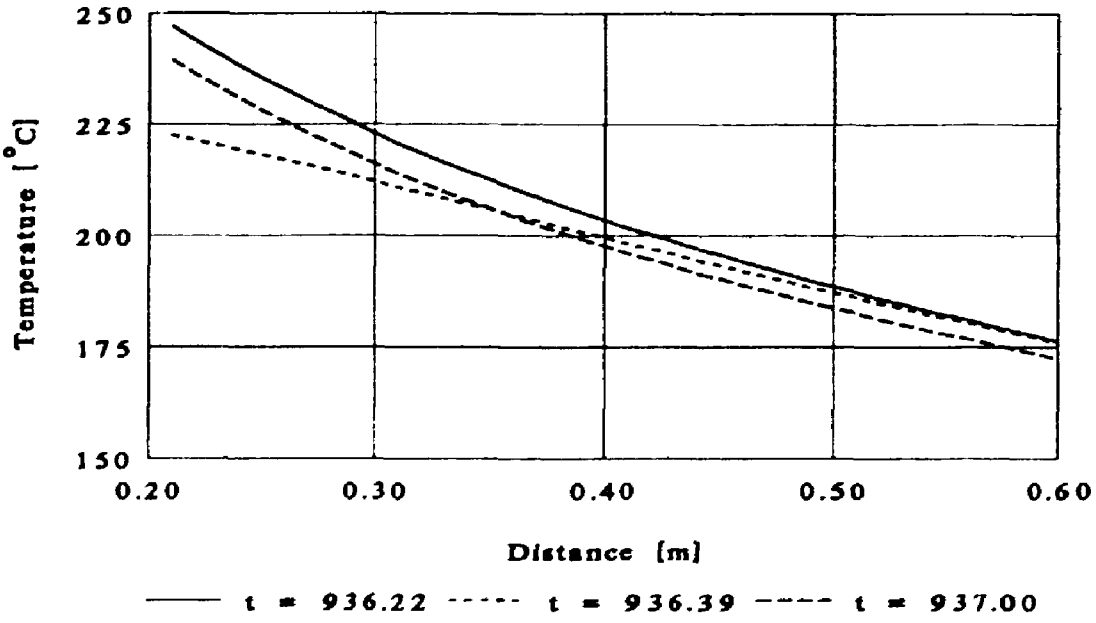

Figure 4.3 Temperature distribution close to the borehole wall at the beginning, at the end and shortly after the heater-interruption.

Table 4.1 Temperature evolution for several calculation points in the case of a constant heat production.

Time [days]	radial coordinate [m]			
	r = .250	r = .366	r = .589	r = .949
680.20	56.51	43.47	36.75	36.01
680.40	73.41	55.06	40.63	36.28
680.60	84.82	64.22	45.42	37.19
680.80	93.38	71.56	50.05	38.61
681.00	100.23	77.64	54.31	40.30
682.00	122.31	98.03	70.59	49.41
685.00	152.42	127.17	96.81	69.51
692.00	179.93	154.28	122.79	92.78
750.00	219.80	193.98	161.95	130.60
936.22	235.31	209.47	177.40	145.94
936.39	235.31	209.48	177.41	145.95
937.00	235.33	209.50	177.43	145.97
945.00	235.60	209.76	177.69	146.23
1000.00	237.13	211.30	179.23	147.76
1100.00	239.12	213.28	181.21	149.74
1200.00	240.50	214.66	182.59	151.12

Table 4.2 Temperature evolution for several calculation points in the case of a heater-interruption.

Time [days]	radial coordinate [m]			
	r = .250	r = .366	r = .589	r = .949
936.22	235.31	209.47	177.40	145.94
936.26	234.25	209.43	177.41	145.95
936.30	229.62	208.63	177.40	145.95
936.34	224.30	206.81	177.32	145.95
936.39	218.13	203.88	176.99	145.95
937.00	228.02	203.23	173.49	145.77
945.00	234.99	209.16	177.11	145.71
1000.00	237.09	211.25	179.18	147.72
1100.00	239.10	213.27	181.20	149.73
1200.00	240.49	214.66	182.58	151.11

5 RESULTS OF THE STRUCTURAL ANALYSIS

5.1 Introduction

The finite element analyses that are performed can be divided in several parts:

1) Linear elastic solution at $t = 0$.
2) Isothermal creep analysis with an empty borehole until $t = 675$ days.
3) The borehole filled with the tube and an isothermal creep analysis until $t = 680$ days.
4) Thermally accelerated creep analysis until $t = 936.22$ days.
5) Heater-interruption of approximately 4 hours until $t = 936.39$ days.
6) Thermally accelerated creep analysis until $t = 1200$ days.

5.2 Linear elastic solution

The initial elastic stress distribution and the radial displacement of the borehole wall can be compared with an analytical solution of a thick-walled cylinder with an infinitely large outer radius [5,8,9]

$$\sigma_{rr} = p\left(\frac{r}{a}\right)^{-2} - p\,, \quad \sigma_{\theta\theta} = -p\left(\frac{r}{a}\right)^{-2} - p\,, \quad \sigma_{zz} = -p\,,$$
$$\sigma_{eq} = p\sqrt{3}\left(\frac{r}{a}\right)^{-2}\,, \quad u(a) = -\frac{3pa}{2E} + \nu\frac{w_0}{h}a = 0.54 \text{ mm} \tag{10}$$

A numerical value $u(a) = 0.6$ mm was obtained. The difference of about 10% can be explained by the finite thickness $b - a$ of the salt volume.

Table 5.1 Linear elastic stress solutions for the model.

r [m]	σ_{rr} [MPa]		$\sigma_{\theta\theta}$ [MPa]		σ_{eq} [MPa]	
	ANSYS	theory	ANSYS	theory	ANSYS	theory
0.26	- 1.04	- 1.02	-21.00	-21.17	17.29	17.28
0.29	- 2.77	- 2.75	-19.27	-19.25	14.29	14.28
0.32	- 4.20	- 4.19	-17.83	-17.81	11.81	11.80
0.35	- 5.38	- 5.37	-16.65	-16.63	9.76	9.75
0.38	- 6.35	- 6.35	-15.67	-15.65	8.07	8.06
0.47	- 7.83	- 7.82	-14.19	-14.18	5.51	5.51
0.56	- 8.83	- 8.83	-13.18	-13.17	3.76	3.76
1.33	-10.61	-10.61	-11.39	-11.39	0.68	0.68
2.35	-10.88	-10.88	-11.13	-11.12	0.22	0.22
5.04	-10.97	-11.00	-11.03	-11.03	0.05	0.05
8.93	-10.99	-11.00	-11.01	-11.01	0.01	0.01
23.15	-11.00	-11.00	-11.00	-11.00	0.00	0.00

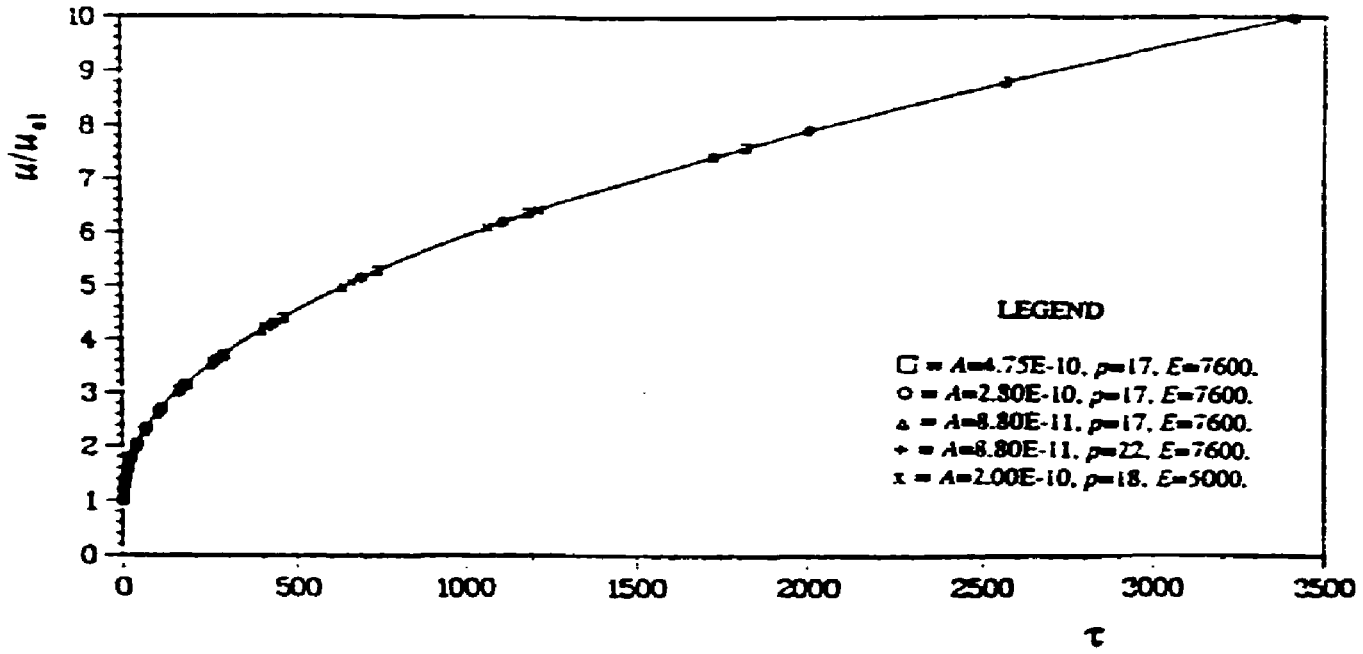

Figure 5.1 Normalized total radial displacement of an infinitely thick cylinder with internal pressure $-p$ (plane strain $n = 5.5$).

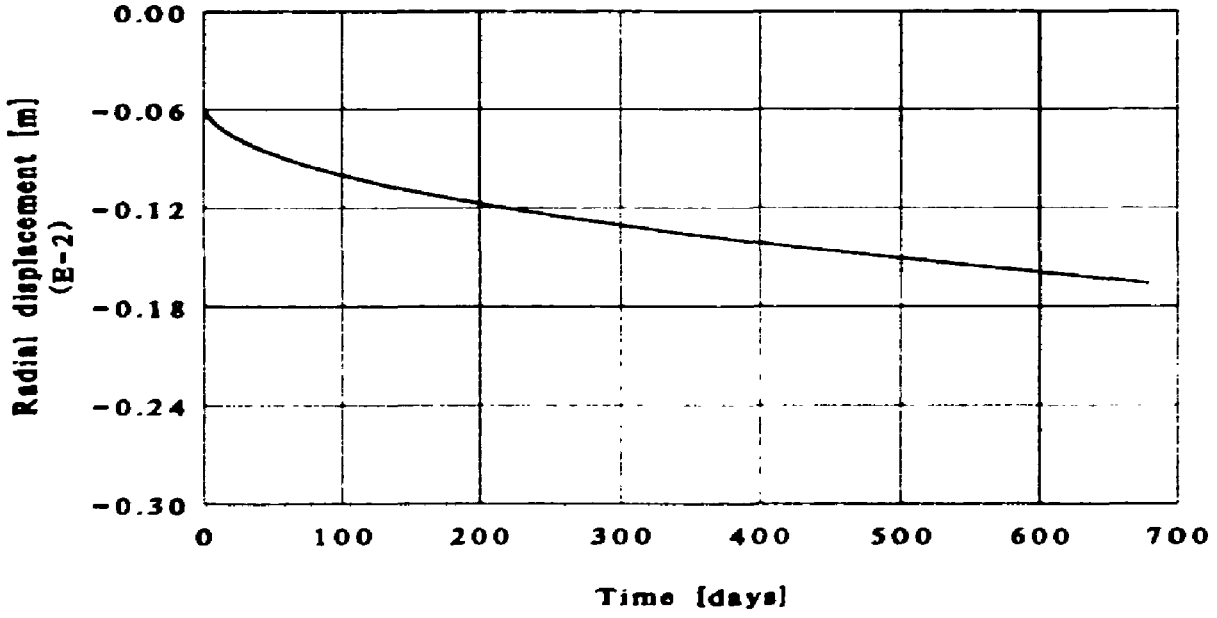

Figure 5.2 Evolution of the radial displacement of the wall in the B-type borehole during the isothermal period.

In Table 5.1 the stresses according to formula (10) as well as the ANSYS results are presented. It can be seen that the finite element result of the initial elastic stress distribution matches the theoretical solution very well.

5.3 Isothermal creep analyses

After 680 days the stationary stress distribution and the stationary displacement rate of the borehole wall have not yet been reached. For the transient state, which is the intermediate stage between the elastic solution and the ultimate stationary solution, there is no analytical solution available. However, in [5] it is shown that the accuracy of the isothermal creep solution of the B-type borehole can be checked by comparing the radial deformation of the borehole wall with the normalized radial displacement $\hat{u}$ of the borehole wall which is only dependent on a normalized time τ and the creep exponent n:

$$\hat{u}(a,\tau) = \frac{u(a,\tau)}{u^{el}(a)} \text{ , where } d\tau = EA\left(\frac{p\sqrt{3}}{1-(b/a)^{-2}}\right)^{n-1} dt \qquad (11)$$

where u^{el} is the elastic radial displacement. In Fig. 5.1 this relation is depicted and it appears that the calculated radial displacement at the borehole wall fulfils this relation.
In Fig. 5.2 the radial displacement at the borehole wall is presented. The results of the A-type borehole are identical with the B-type borehole for the first 675 days, when the backfilling of the annular gap between liner and borehole wall is started.

5.4 Thermally accelerated creep analyses

After 680 days the heat generation is started. The nodal temperatures are calculated with the computer code TASTE (see chapter 2). The radial displacement at the borehole wall is presented in Fig. 5.3 for both types of boreholes, while the radial displacement of the outer radius of the steel liner is given in Fig. 5.4. It is shown that when the salt is heated the annular empty space will be filled with salt very rapidly. After about 12 days of heat generation the salt and the steel make contact. In both boreholes the steel expands as a result of the large temperature gradient and the salt creeps in the direction of the liner. After the physical contact with the salt the steel is pushed back a little and from this moment the radial displacement of the borehole wall and of the steel show the same tendency.
Fig. 5.5 and 5.6 show the radial, tangential and equivalent stresses in the salt for the A-type borehole, while Fig 5.7 and 5.8 do so for the B-type borehole. For both types of boreholes considered the start of the heat generation leads to an increase of the equivalent stress. This is a thermal effect dominating the creep mechanism. Since the temperatures are increasing the thermally accelerated creep mechanism starts to dominate leading to a stress relaxation. This decrease in equivalent stress occurs more rapidly in case of the A-type borehole because a hydrostatic stress state can be reached sooner because of the presence of the porous medium.
The pressure load from the salt on the steel liner for both types of boreholes is again presented in Fig. 5.9 and tabulated in Table 5.1. A maximum pressure load working on the steel liner of 23.6 MPa was found after 30 days of heating in the A-type borehole. In the B-type borehole a maximum pressure load of 20.1 MPa was found 150 days after the heaters were started. The differences in pressure loads are caused by the presence of the porous medium between the steel liner and the borehole wall. In the case of the B-type borehole the salt creeps very rapidly in the empty annular gap leading to a slower built-up of the pressure load than in the case of the A-type borehole, where the creep of the salt is hampered by the presence of the porous medium. Therefore, the maximum load of the A-type borehole is

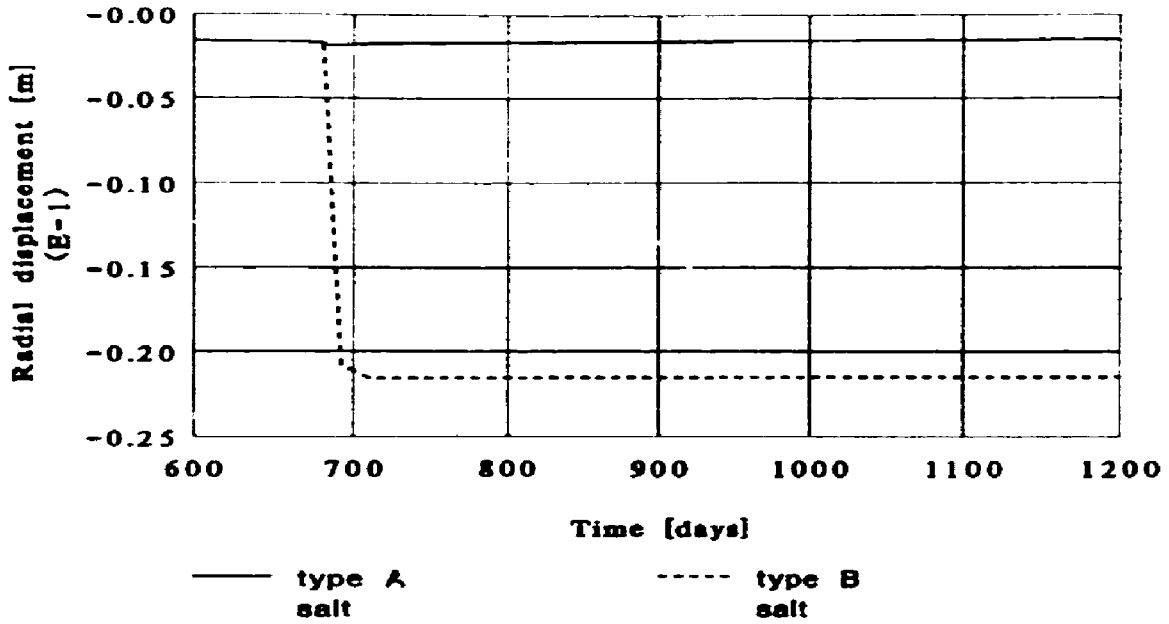

Figure 5.3 Evolution of the radial displacement of the salt at the heated borehole wall.

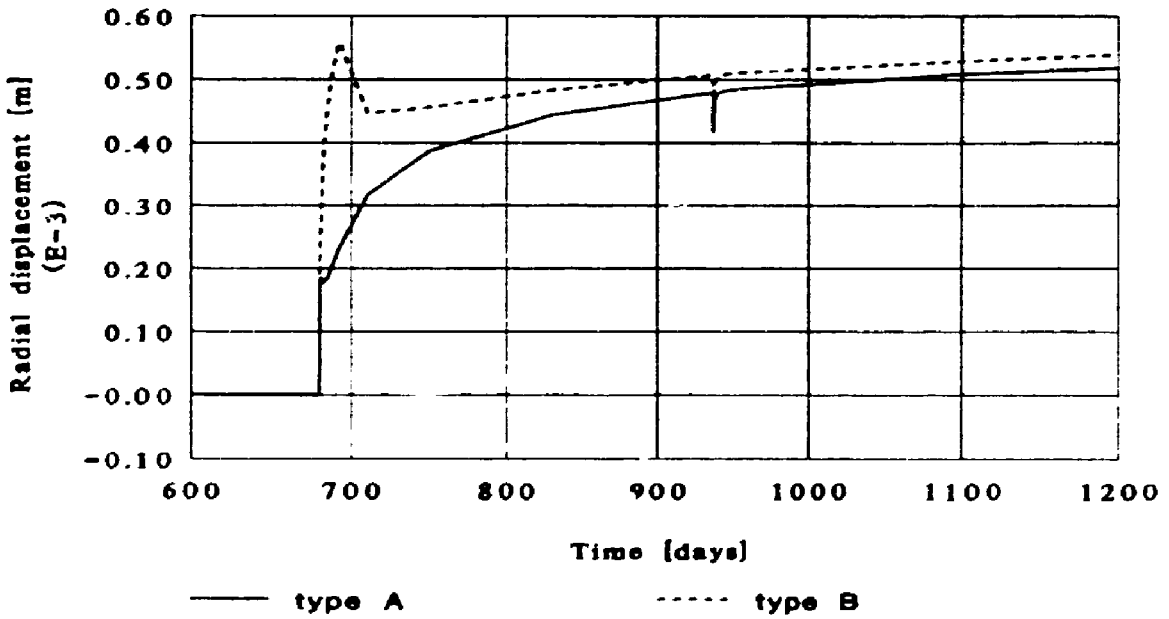

Figure 5.4 Evolution of the radial displacement of the inner radius of the heated steel liner.

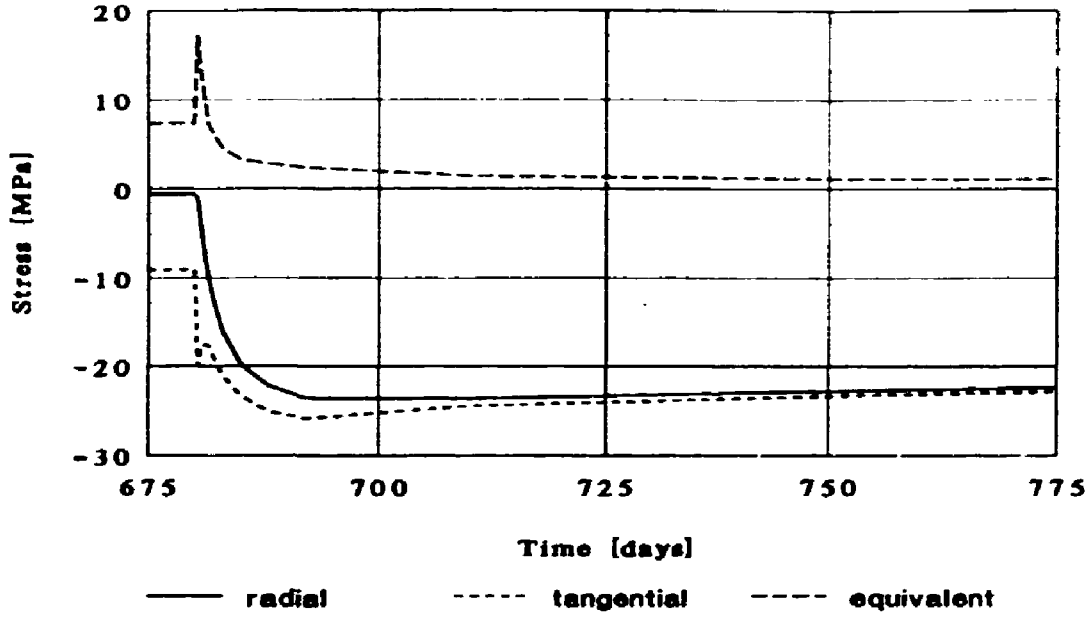

Figure 5.5 Evolution of the stresses in the salt at the borehole wall in the case of the A-type borehole (from t = 675 to t = 775 days).

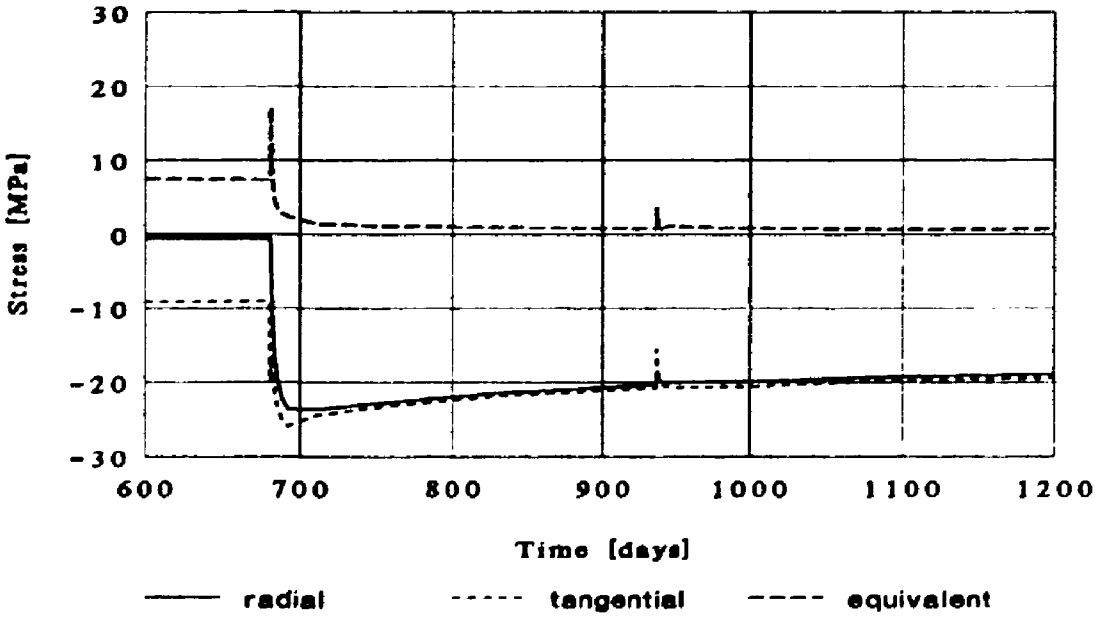

Figure 5.6 Evolution of the stresses in the salt at the borehole wall in the case of the A-type borehole (from t = 600 days until t = 1200 days).

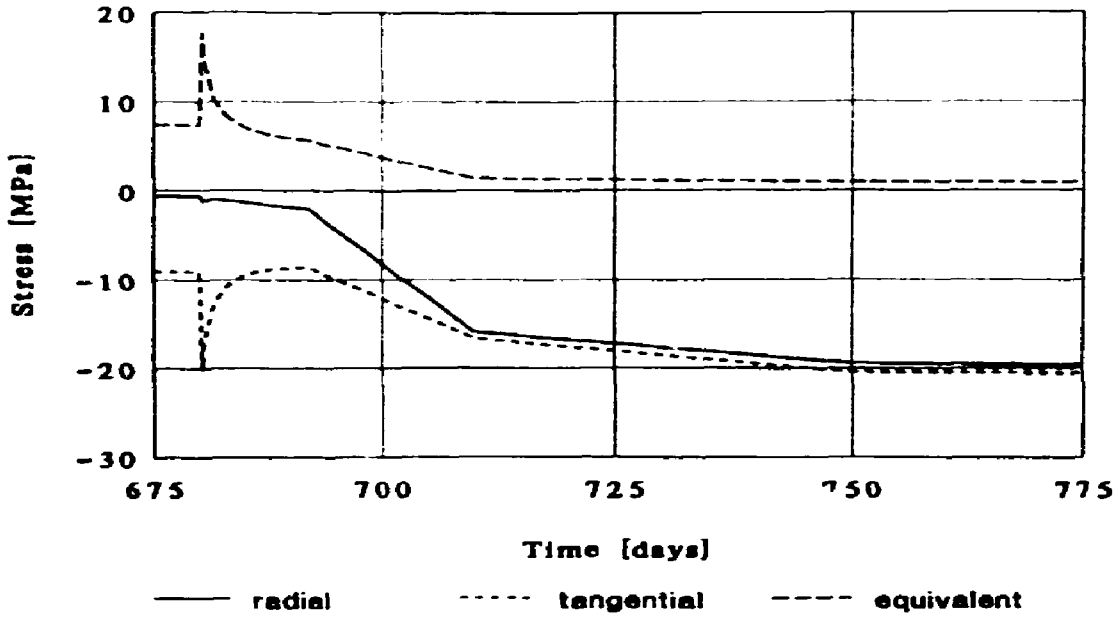

Figure 5.7 Evolution of the stresses in the salt at the borehole wall in the case of the B-type borehole (from t = 675 days to t = 775 days).

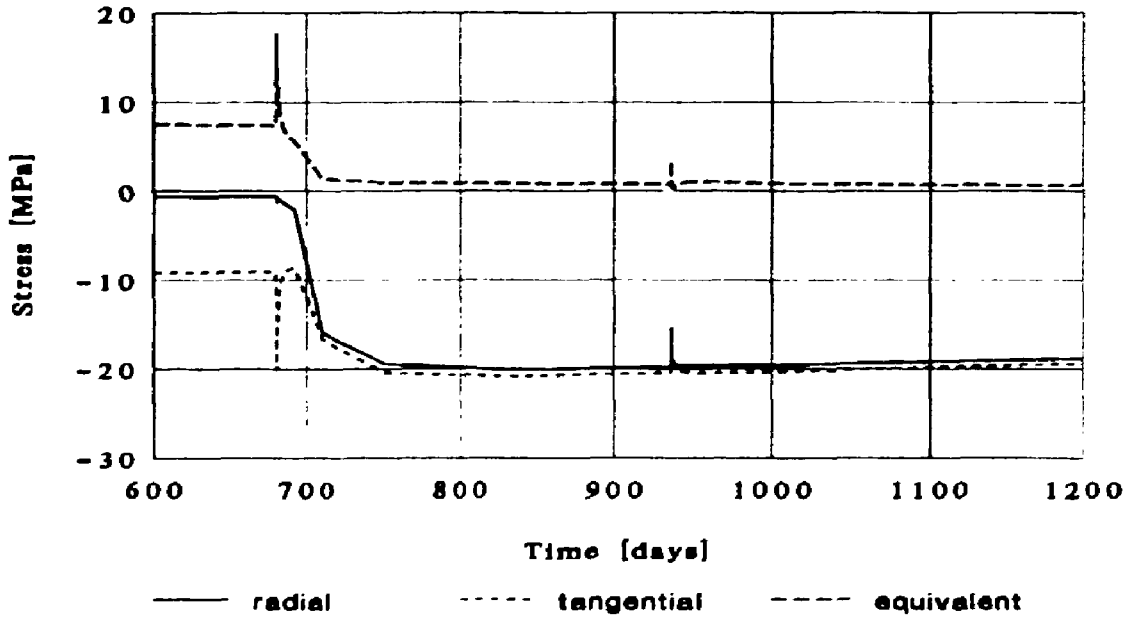

Figure 5.8 Evolution of the stresses in the salt at the borehole wall in the case of the B-type borehole (from t = 675 days until t = 1200 days).

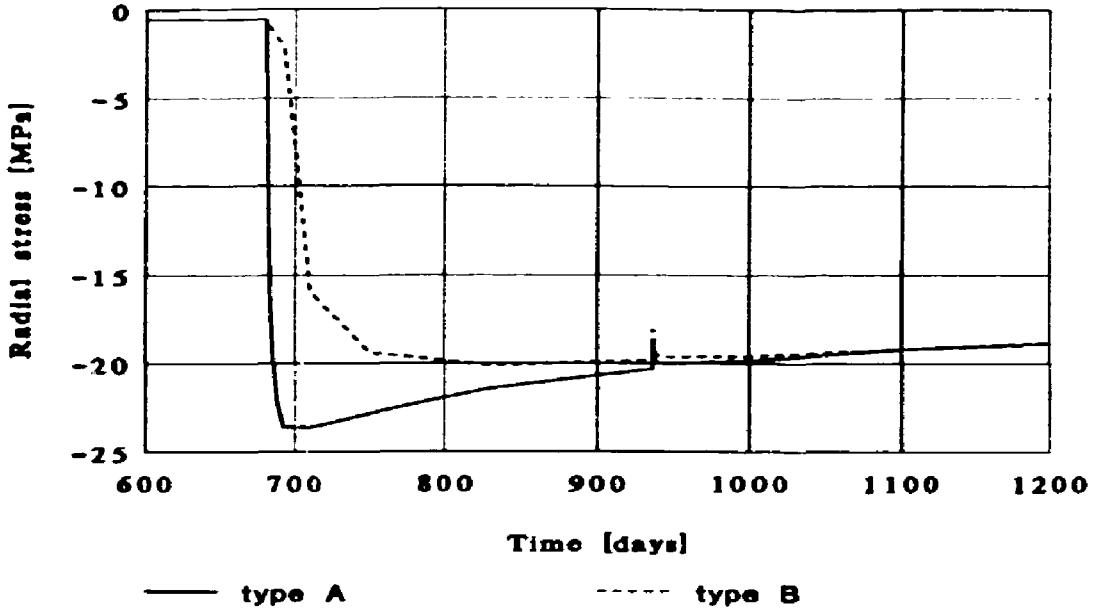

Figure 5.9 Evolution of the pressure load of the heated salt working on the steel liner.

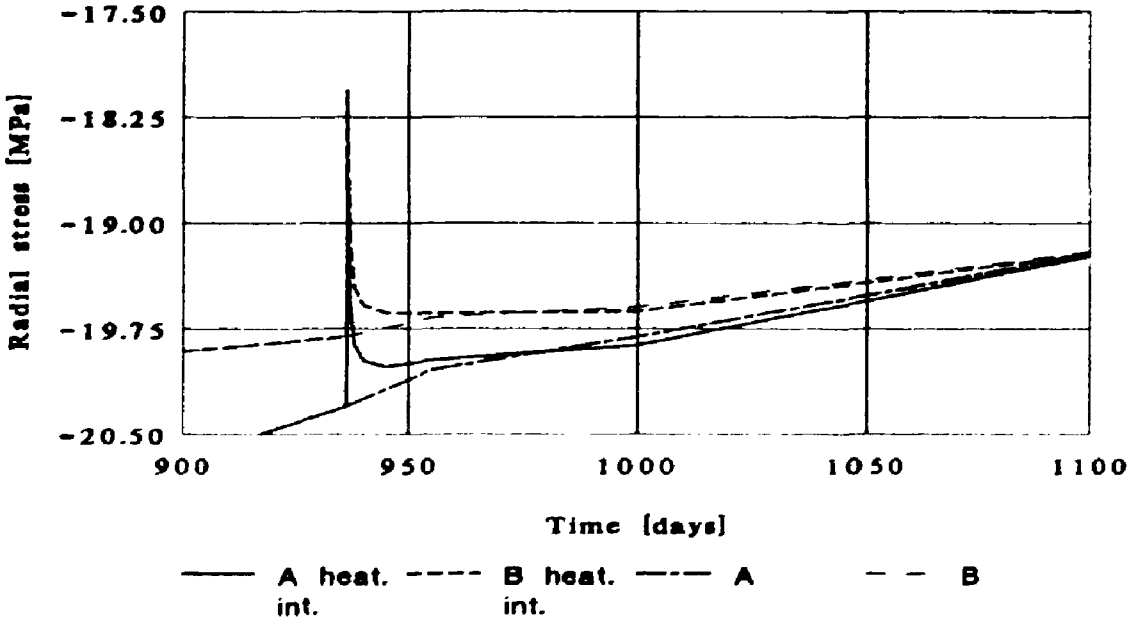

Figure 5.10 Drop in the pressure load of the heated salt working on the steel liner during the heater-interruption.

Table 5.1 Pressure load from the salt on the steel liner.

Time after excavation [days]	pressure load [MPa]			
			heat.-int.	
	A	B	A	B
680.00	- 0.55	- 0.55	- 0.55	- 0.55
680.20	- 0.97	- 0.97	- 0.97	- 0.97
680.40	- 1.59	- 1.17	- 1.59	- 1.17
680.60	- 3.31	- 1.05	- 3.31	- 1.05
680.80	- 4.96	- 1.03	- 4.96	- 1.03
681.00	- 6.45	- 1.01	- 6.45	- 1.01
682.00	-12.43	- 1.00	-12.43	- 1.00
683.00	-15.99	- 1.07	-15.99	- 1.07
685.00	-19.83	- 1.29	-19.83	- 1.29
688.00	-22.29	- 1.64	-22.29	- 1.64
710.00	-23.62	-15.90	-23.62	-15.90
750.00	-22.83	-19.41	-22.83	-19.41
830.00	-21.41	-20.12	-21.41	-20.12
936.22	-20.30	-19.81	-20.30	-19.81
936.26	-20.12	-19.57	-19.98	-19.57
936.30	-20.12	-19.73	-19.55	-19.09
936.34	-20.12	-18.72	-19.11	-18.60
936.39	-20.12	-18.72	-18.61	-18.05
937.00	-20.12	-19.72	-19.57	-19.13
938.00	-20.11	-19.72	-19.86	-19.45
940.00	-20.10	-19.71	-19.98	-19.58
945.00	-20.09	-19.70	-20.02	-19.64
955.00	-20.04	-19.67	-19.97	-19.64
1000.00	-19.81	-19.59	-19.87	-19.62
1100.00	-19.21	-19.20	-19.23	-19.22
1200.00	-18.90	-18.99	-18.90	-18.83

higher and is reached sooner than the B-type borehole. In Fig. 5.10 the drop in pressure load is compared with the calculated tube loads for the boreholes with the continuous heat generation. The heater-interruption (cf. Fig 5.10) leads to a reduction of the pressure load because the thermal contribution of the stress decreases. At the end of the heater interruption pressure drops of 1.69 MPa and 1.76 MPa are reached for the A-type and B-type borehole, respectively. About 160 days after the reparation of the heaters (at t = 1100 days) the tube load will have been rehabilitated for both types of boreholes considered and the differences in tube load are negligible.

The hoop stress in the steel is presented in Fig. 5.11. As has been previously stated, after about 12 days the salt and the steel make contact in the B-type borehole and the following expression is valid:

$$s_{\theta\theta} = \frac{\sigma_r(a)\,c}{d - c} \qquad (12)$$

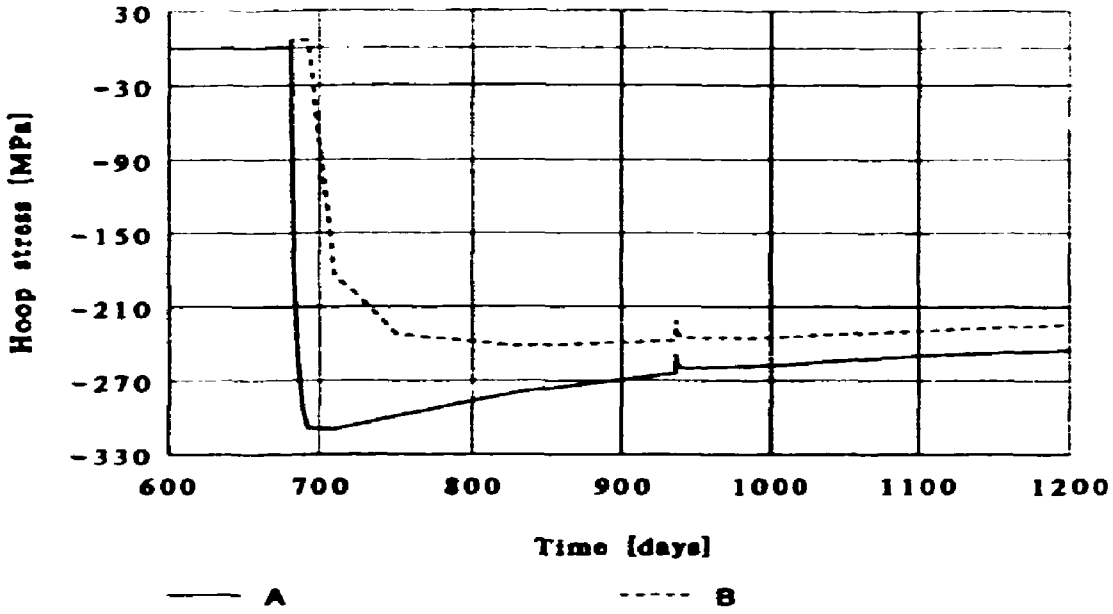

Figure 5.11 Evolution of the hoop stress in the steel.

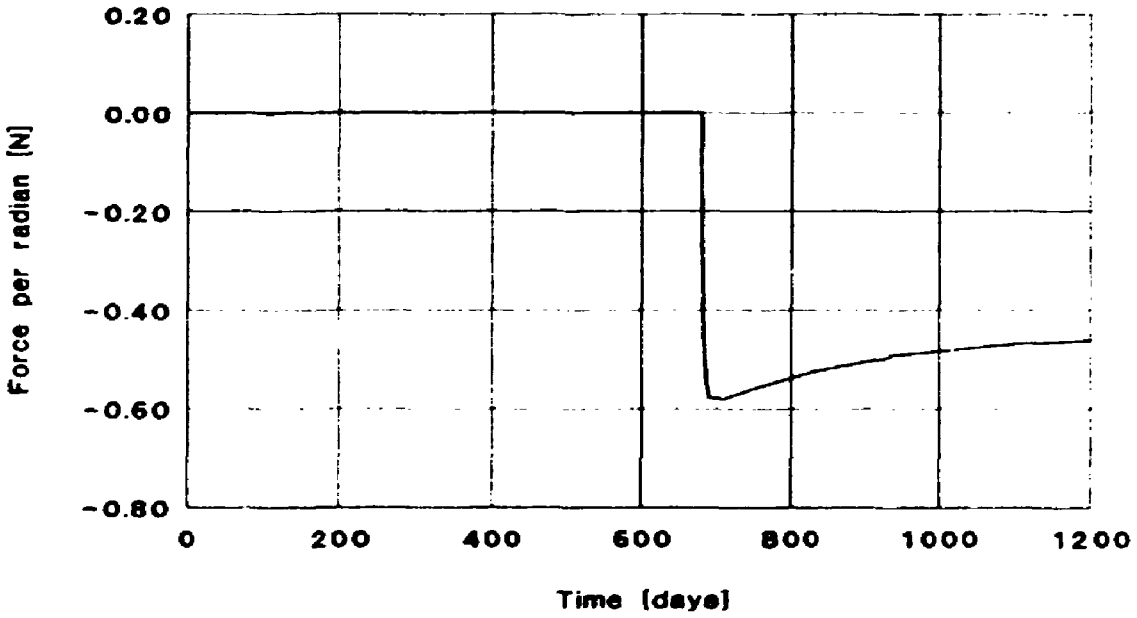

Figure 5.12 Force per radian working on the porous medium.

where $s_{\theta\theta}$ denotes the hoop stress in the steel. In the case of the A-type borehole the evolution of the hoop stress in the salt and in the steel show the same tendency after about 20 days of heat generation when the porous medium is not compressed any further.
The force per radian working on the porous medium is given in Fig. 5.12 while the radial compression is Fig. 5.13, respectively. It is clear that after 12 days of heat generation the porous medium is not compressed any further. A stiffness of less than 20% of the salt stiffness is reached.

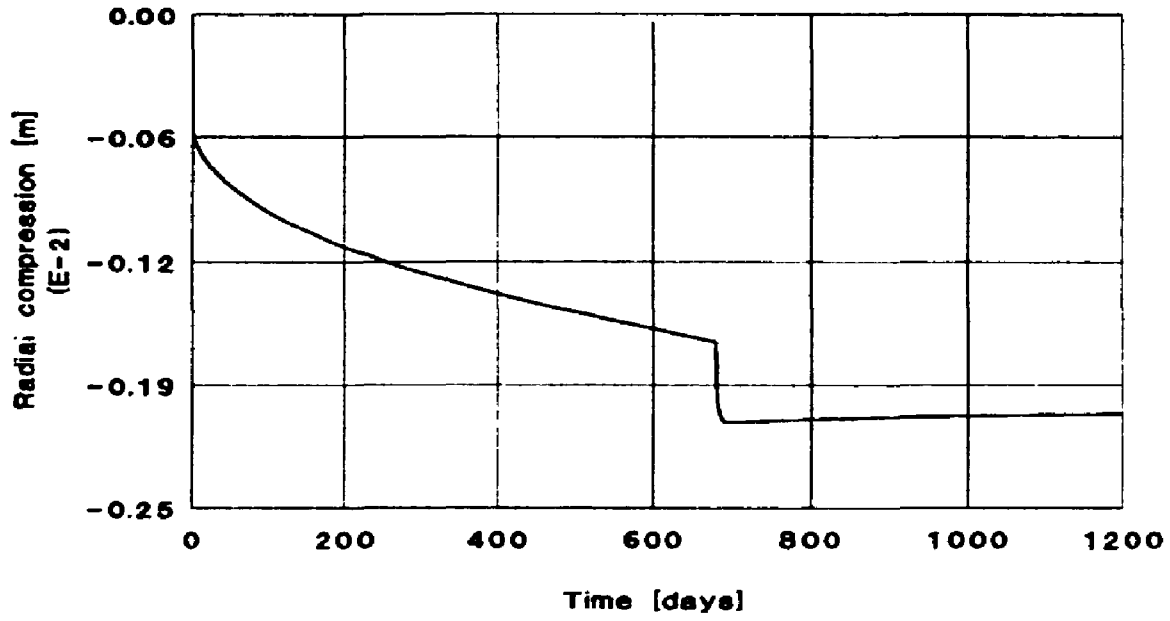

Figure 5.13 Radial compression in the porous medium.

6 CONCLUSIONS

Temperature calculations and finite element analyses of the HAW field including an internal borehole have been performed. Two axisymmetrical models including one borehole of type A and B, respectively, are made in order to simulate a heater-interruption. It is concluded that:

- Maximum pressure loads of 23.6 MPa and 20.1 MPa were found after 12 days and 150 days of heating at the steel liner in the A-type and B-type boreholes, respectively. The maximum pressure load of the heated A-type borehole is higher and is reached sooner than that of the heated B-type borehole because of the presence of the porous medium between the steel liner and the borehole wall.

- A heater-interruption of approximately 4 hours during which the power is reduced from 9600 W to zero leads to a temperature drop of 17°C.

- During this heater-interruption a maximum pressure drop of about 1.76 MPa was obtained for both types of boreholes.

- About 20 days after reparation of the heaters the differences in evolution of the maximum temperature and the maximum tube load with the corresponding evolutions during a continuous heat-production will be negligible.

REFERENCES

[1] Das HAW-project, Demonstrationseinlagerung hochradioaktiver Abfalle in Salzbergwerk ASSE, 2. Halbjahresbericht 1986.

[2] Das HAW-project, Demonstrationseinlagerung hochradioaktiver Abfalle in Salzbergwerk ASSE, Jahresbericht 1987.

[3] van den Horn, B. A., Hamilton, L. F. M., Prij J.:
Thermo-mechanical pre-test analyses for the HAW test field, part 9.
Restricted distribution report ECN-89-167.

[4] Jong, C.J.T., Kevenaar, J.W.A.M.:
TASTE, Three-dimensional analysis of salt dome temperatures, ECN-82-18, December 1982.

[5] Prij, J.:
On the design of a radioactive waste repository, PhD Thesis, University of Twente, June 1991.

[6] ANSYS Engineering Analysis System Swanson Analysis System Inc. Houston, Pennsylvania, 15342 (U.S.A.).

[7] Prij, J., Hamilton, L. F. M., Beemsterboer, C.J.J., van den Horn, B. A.:
Thermo-mechanical pre-test analyses for the HAW test field, ECN-R-91-001, (1991).

[8] Besseling, J.F.:
Numerical methods in stress analysis. Introduction to Creep and Plasticity, Université Libre de Bruxelles, Faculté des Sciences Appliqués (1968).

[9] Timoshenko, S.:
Strength of Materials, part 2, D. van Nostrand Comp. Inc., Princeton (1956).

APPENDICES

Appendix A Non-linear force-deflection element

In this appendix the method of taken into account the stiffness of the porous medium is elucidated. First consider a rigid cylindrical beam with length h surrounded by a concentric elastic cylinder with inner radius d and outer radius a loaded by a uniform pressure p (cf. Fig. A.1). Under plane strain conditions we have one degree of freedom, viz. the radial displacement $u(r)$. In the case of infinitesimal displacements the kinematical relation between the strains and the displacements in the elastic medium are

$$\varepsilon_{rr} = \frac{du}{dr} \quad , \quad \varepsilon_{\theta\theta} = \frac{u}{r} \tag{13}$$

The constitutive relations given by Hooke's Law are

$$\sigma_{rr} = \frac{E}{1-\nu^2}(\varepsilon_{rr} + \nu\,\varepsilon_{\theta\theta}) \quad , \quad \sigma_{\theta\theta} = \frac{E}{1-\nu^2}(\varepsilon_{\theta\theta} + \nu\varepsilon_{rr}) \tag{14}$$

The radial stress σ_{rr} and the hoop stress $\sigma_{\theta\theta}$ have to satisfy equilibrium:

$$\frac{d\sigma_{rr}}{dr} + \frac{\sigma_{rr} - \sigma_{\theta\theta}}{r} = 0 \tag{15}$$

Substituting equation (13) into (14) and (14) into (15) leads to the following differential equation for the radial displacement

$$\frac{d^2u}{dr} - \frac{1}{r}\frac{du}{dr} + \frac{u}{r^2} = 0 \tag{16}$$

with solution

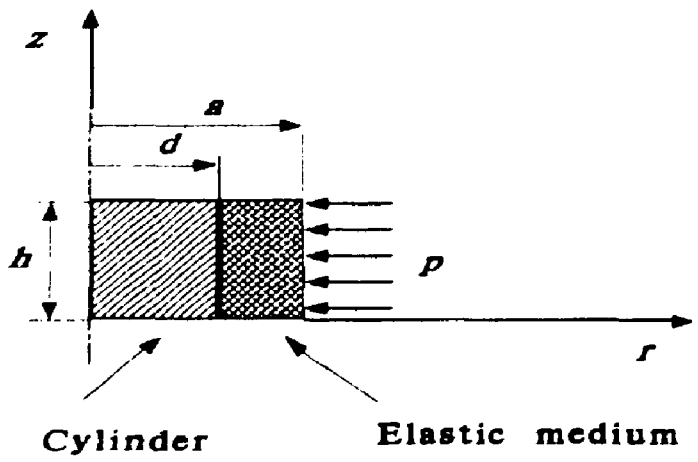

Figure A.1 Rigid cylindrical beam surrounded by an elastic medium.

$$u(r) = \frac{p(1-\nu^2)}{E}\left[\frac{a^2}{d^2(\nu-1)-a^2(\nu+1)}\right]\left(r-\frac{d^2}{r}\right) \tag{17}$$

satisfying the boundary conditions

$$\sigma_{rr}(a) = -p \quad , \quad u(d) = 0 \tag{18}$$

The force per radian F necessary to deform the elastic medium can be expressed in the pressure p

$$F = -pah \tag{19}$$

The relation between the deflection $u(a)$ and the force F is given by

$$F = \frac{Eh}{(1-\nu^2)}\left[\frac{d^2(\nu-1)-a^2(\nu+1)}{a^2-d^2}\right]u(a) \tag{20}$$

In the case of the borehole of type A the compressing force working on the porous medium must be divided over the two non-linear force-deflection elements. The stiffness E_p of the porous medium is given by

$$E_p = Ef\left(\frac{\Delta V}{V}\right) \tag{21}$$

where f is a function of the volume strain $\Delta V/V$ of the porous medium (cf. Fig. 3.2). The volume strain can be expressed in terms of the radial displacements $u(d)$ and $u(a)$ of the inner and outer radius, respectively, of the porous medium:

$$\frac{\Delta V}{V} = \frac{(a+u(a))^2-(d+u(d))^2-(a^2-d^2)}{a^2-d^2} \approx \frac{2d(u(a)-u(d))}{a^2-d^2} \tag{22}$$

So in both non-linear force-deflection elements the following relation holds

$$F = \frac{Eh(u(a)-(d))}{2(1-\nu^2)}\left[\frac{d^2(\nu-1)-a^2(\nu+1)}{a^2-d^2}\right]\beta(u(a)-u(d)) \tag{23}$$

where $\beta(u)$ is a stiffness reduction factor dependent on the deformation. The deflection $u(a) - u(d)$ is called the stretch of the porous medium. Equation (23) is depicted in Fig. A.2. In Fig. A.3 the FEM results are presented. It appears that the force and deflection are accurately calculated.

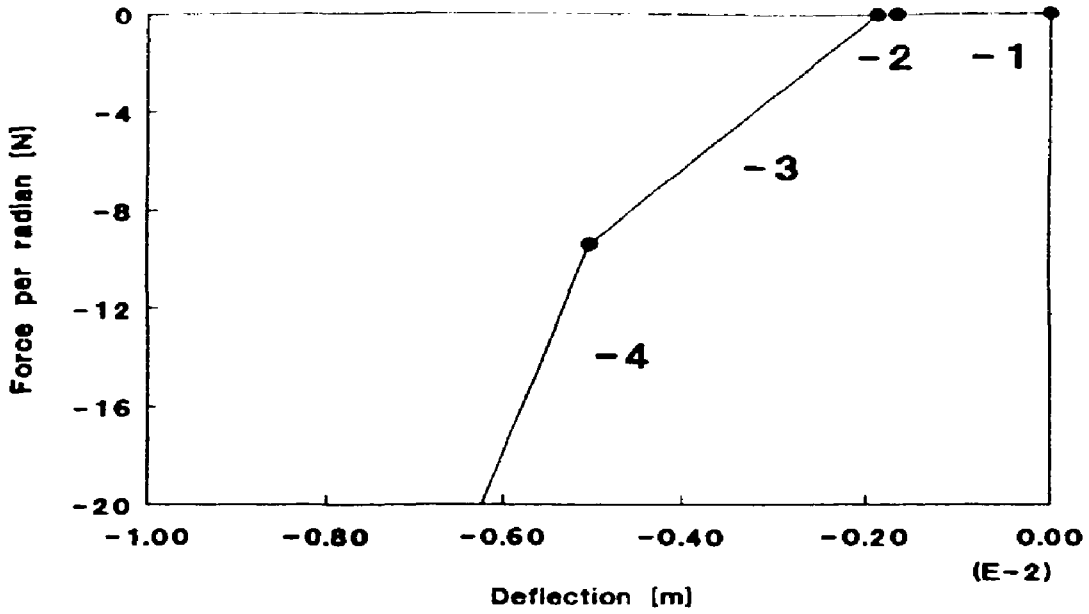

Figure A.2 Nonlinear force-deflection diagram of the spring element STIFF 39.

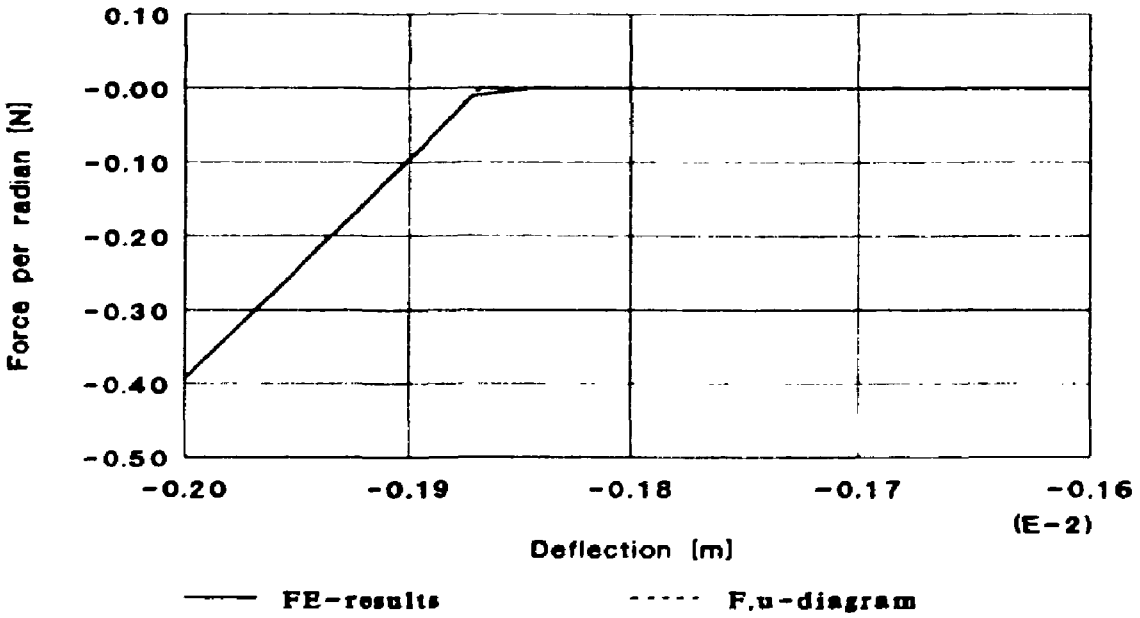

Figure A.3 Nonlinear force-deflection diagram and FE-results of the spring element STIFF 39.

Appendix B Magnetic tapes

The analysis files are stored on a 9 track 6250 BPI tape, created with the BACKUP-utility on the CONVEX. The VSN number of the tape is 1715 and the tape has no password. The name of each file includes all the necessary information about the contents. All the results of the analyses with the heater-interruption are stored on the directories boreholeA and boreholeB, while the analyses with constant heat generation are stored on the directories nhiboreholeA and nhiboreholeB. For example:

Files	Description
/boreholeA/start	jobfile elastic and creep analysis until t = 680 days
/boreholeA/restart	jobfile creep analysis until t = 1200 days
/boreholeA/post26/file12.dat	postfile from t = 0 until t = 1200 days
/boreholeA/printdir/startprint	printout for jobfile start
/boreholeA/printdir/restartprint	printout for jobfile restart
/boreholeA/histdir/starthist	historyfile generated in start
/boreholeA/histdir/restarthist	historyfile generated in restart